The Astrophysical Journal, 710:1619–1626, 2010 February 20 doi:10.1088/0004-637X/710/2/1619

CONVECTION THEORY AND SUB-PHOTOSPHERIC STRATIFICATION

David Arnett[1], Casey Meakin[1], and Patrick A. Young[1,2]
[1] Steward Observatory, University of Arizona, 933 North Cherry Avenue, Tucson, AZ 85721, USA;
darnett@as.arizona.edu, casey.meakin@gmail.com, patrick.young.1@asu.edu
[2] School of Earth and Space Exploration, Arizona State University, Tempe, AZ 85287-1404, USA
Received 2009 October 4; accepted 2010 January 2; published 2010 February 2

ABSTRACT

As a preliminary step toward a complete theoretical integration of three-dimensional compressible hydrodynamic simulations into stellar evolution, convection at the surface and sub-surface layers of the Sun is re-examined, from a restricted point of view, in the language of mixing-length theory (MLT). Requiring that MLT use a hydrodynamically realistic dissipation length gives a new constraint on solar models. While the stellar structure which results is similar to that obtained by Yale Rotational Evolution Code (Guenther et al.; Bahcall & Pinsonneault) and Garching models (Schlattl et al.), the theoretical picture differs. A new quantitative connection is made between macro-turbulence, micro-turbulence, and the convective velocity scale at the photosphere, which has finite values. The "geometric parameter" in MLT is found to correspond more reasonably with the thickness of the superadiabatic region (SAR), as it must for consistency in MLT, and its integrated effect may correspond to that of the strong downward plumes which drive convection (Stein & Nordlund), and thus has a physical interpretation even in MLT. If we crudely require the thickness of the SAR to be consistent with the "geometric factor" used in MLT, there is no longer a free parameter, at least in principle. Use of three-dimensional simulations of both adiabatic convection and stellar atmospheres will allow the determination of the dissipation length and the geometric parameter (i.e., the entropy jump) more realistically, and *with no astronomical calibration.* A physically realistic treatment of convection in stellar evolution will require substantial additional modifications beyond MLT, including nonlocal effects of kinetic energy flux, entrainment (the most dramatic difference from MLT found by Meakin & Arnett), rotation, and magnetic fields.

Key words: binaries: eclipsing – convection – hydrodynamics – stars: atmospheres – stars: evolution – Sun: photosphere – white dwarfs

Online-only material: color figures

1. INTRODUCTION

Recent simulations of three-dimensional compressible convection and their theoretical analysis (Meakin & Arnett 2007b; Arnett et al. 2009) have shown that the interpretation of mixing-length theory (MLT), as currently used in stellar evolution (Böhm-Vitense 1958; Cox 1968; Clayton 1983; Hansen & Kawaler 1994; Kippenhahn & Weigert 1990) is flawed. This mixing length ℓ is parameterized as $\alpha_{\rm ML} = \ell/H_P$, where H_P is the local pressure scale height, and $\alpha_{\rm ML}$ is adjusted to reproduce the radius of the present-day Sun. However, instead of being an adjustable parameter, the mixing length is found to correspond to the dissipation length ℓ_d of the turbulence (Kolmogorov 1941, 1962), and determined by the size of the largest eddies (Meakin & Arnett 2007b; Arnett et al. 2009). From our own simulations (Meakin & Arnett 2010a, 2010b) and those of others, we find a robust tendency for the dissipation length to be

$$\ell_d \approx \min(\ell_{\rm CZ}, 4H_P), \quad (1)$$

where $\ell_{\rm CZ}$ is the depth of the convection zone (Arnett et al. 2009). For shallow convection zones, the dissipation length is limited by the depth of the convective region and seems to approach a limiting value of $\ell_d \approx 4H_P$ for deep convection zones. In this paper, we examine the consequence of such a mixing length within the standard MLT formulation.

If $\alpha_{\rm ML}$ is fixed, other parameters in MLT, which are generally left fixed by historical convention, may be adjusted to compensate (e.g., Tassoul et al. 1990; Salaris & Cassisi 2008). The most significant of these parameters is the geometric factor,[3] which adjusts the rate at which radiation limits the degree of entropy excess in the superadiabatic region (SAR). For simplicity, we use $g_{\rm ML}$ to denote the geometric factor in units of the value used in conventional MLT (see the Appendix for details). If we identify the geometric parameter as a measure of the thickness of the SAR, we remove the last free parameter in MLT.[4] Although MLT is an incomplete theory, it does serve as a useful and well-known "language" to explain some of the changes implied by three-dimensional simulations.

The MLT itself (Vitense 1953; Böhm-Vitense 1958), if used consistently, does capture some aspects of turbulent convection. This, and its freely adjusted parameter α (which allows fitting of observations), are reasons for its wide use. However, a real replacement for MLT will supply missing terms in the theoretical formulation (Arnett et al. 2009) and provide a global solution which relaxes the *local* connection between the superadiabatic gradient and the enthalpy flux, so that regions of the convective zone can be subadiabatic, as observed in simulations.

In order to establish a "baseline" from which to compare new effects demanded by numerical simulations and by laboratory experiment (e.g., fluctuations, non-locality, and entrainment),

[3] This is essentially the *c* factor of Tassoul et al. (1990).

[4] The idea of a "blob" size is a misleading aspect of MLT. Stein & Nordlund (1998) and Nordlund et al. (2009) do not find such a feature, but do find a SAR which has an average thickness of less than a pressure scale height. The relevant width is probably smaller because a pronounced corrugation "smears" the width upon averaging. The "blob" size is best thought of as a parameter in one dimension which gives a net effect on entropy change which is similar to that of an integral over trajectories in three dimensions, averaged over time and space. A quantitative connection between the "blob" size and three-dimensional simulations remains to be made; here, we merely force self-consistency in one dimension. We take the thickness of the SAR to be the full width at half-maximum, and it should approximately equal the diameter of a "blob" in MLT.

Table 1
Mixing Length Parameters[a]

MLT Choice	a	b	c	ℓ
BV58[b]	0.125	0.5	24	Free parameter
ML2[c]	1	2	16	Free parameter
AMY[d]	≈0.1	0.256	$24/g_{\rm ML}^{e}$	$\min(4H_P, \ell_{\rm CZ})$

Notes.
[a] As defined in Tassoul et al. (1990).
[b] Böhm-Vitense (1958); this is ML1.
[c] Tassoul et al. (1990) and Salaris & Cassisi (2008).
[d] Arnett et al. (2009), and this paper.
[e] $g_{\rm ML} = (\ell/\sqrt{3}r_b)^2$, where r_b is the radius of a blob just contained inside the SAR.

the framework of the standard solar model (Bahcall et al. 2004) is examined with respect to the modification of some aspects of convection. In this paper, we show that the addition of dynamically realistic values of mixing length and geometric factor give some interesting insights into the nature of the average stratification of the Sun just below the photosphere. In Section 2, we construct a series of solar models with $\alpha_{\rm ML}$–$g_{\rm ML}$ pairs, to delineate their properties. The notion of a "standard solar model" derives from the work of John Bahcall and collaborators, and is summarized in Bahcall (1989). It represents what is probably the most carefully tested aspect of the theory of stellar evolution. In Section 3, we compare our models to standard results using the Yale Rotational Evolution Code (YREC; Guenther et al. 1992; Bahcall & Pinsonneault 2004), and the Garching code (see Schlattl 1996; Schlattl et al. 1997). In Section 4, we compare the outer layers of our models to the three-dimensional atmospheres of Nordlund and Stein (Asplund 2005), semi-empirical models of the solar atmosphere (Fontenla et al. 2006), and re-examine the question of convective velocities at the photosphere. In order that the thickness of the SAR corresponds to the size of the blob used in MLT, i.e., to maintain self-consistency in one dimension, we find that the range of $\alpha_{\rm ML}$–$g_{\rm ML}$ pairs is restricted and is different from MLT values conventionally used. In Section 5, we summarize the implications of this work.

2. SOLAR MODELS

2.1. Hydrodynamically consistent MLT Parameters

Tassoul et al. (1990) have defined the parameters in MLT in a concise way: they define three parameters a, b, and c in terms of an adjustable mixing length, ℓ. In the notation of Arnett et al. (2009), $\Delta\nabla = \nabla - \nabla_e$, so we have

$$a = v_c^2 H_P/\ell^2 g\beta_T \Delta\nabla, \quad (2)$$

$$b = F_c H_P/\rho v_c C_P T \ell \Delta\nabla, \quad (3)$$

and

$$c = C_P \rho^2 \ell v_c \kappa(\nabla_e - \nabla_a)/\sigma T^3 \Delta\nabla. \quad (4)$$

Table 1 gives standard values for the mixing length parameters in the formulation of Tassoul et al. (1990). The first two entries are the standard "flavor" due to Böhm-Vitense (1958), and the ML2 flavor of Tassoul et al. (1990). In both cases, the values of a, b, and c are fixed and the mixing length ℓ adjusted to reproduce the solar radius of the present-day Sun. The third line presents the values of these parameters as estimated from three-dimensional simulations (Meakin & Arnett 2007b; Arnett et al. 2009). Two striking differences are apparent: (1) the mixing length is not an arbitrary constant. For deep convection zones (like the Sun which has $\ell_{\rm CZ} = 20H_P$), the mixing length (dissipation length) approaches $4H_P$. (2) The "c" parameter is intimately related to the geometric factor, and we assume to the thickness of the superadiabatic layer. Both the "a" and "b" parameters are fixed at the values for adiabatic turbulent convection (Arnett et al. 2009), leaving $c = 24/g_{\rm ML}$ as the remaining free parameter. Note that the flavors BV58 (ML1) and ML2 both differ from those suggested by the simulations.

Even though there are additional effects shown in three-dimensional turbulent simulations which are not contained in MLT, it is useful to examine those changes which can be captured with a standard stellar evolution code. If the value of $\alpha_{\rm ML} = \ell/H_P$ is fixed, which of these parameters is to be varied in MLT to get an acceptable solar model? The only parameter sufficient to the task is the "geometric parameter" (i.e., c or $g_{\rm ML}$). A simple way to examine the effects of the geometric parameter is to vary its value relative to the value used in conventional MLT; we denote this scaled value by $g_{\rm ML}$ (see the Appendix). We relate this factor to the thickness of the SAR by $g_{\rm ML} = (\ell_d/\sqrt{3}r_b)^2$, where the "blob diameter" $2r_b$ is the thickness of the SAR (see the previous footnote regarding the interpretation of this "blob" size in one dimensional and three dimensional cases). MLT results if we set $g_{\rm ML} = 1$; this identifies the SAR with the superadiabatic "element" of (Kippenhahn & Weigert 1990, p. 50). In MLT, the "blob" is assumed to have a dimension fixed by the mixing length. This is inconsistent with three-dimensional atmosphere simulations (Stein & Nordlund 1998; Nordlund et al. 2009) and solar models (Guenther et al. 1992; Schlattl et al. 1997 and below), which show that the SAR is much less than four pressure scale heights thick, which is the hydrodynamically inferred dissipation length. MLT has *two* characteristic lengths, one of which is ignored by forcing the geometric parameter lengthscale to be the same as the mixing length (turbulent dissipation length). We will allow the "blob" size to differ from the mixing length in order to vary $g_{\rm ML}$.

For theoretical clarity, we will apply radiative diffusion theory consistently up to the photosphere. While radiation transfer theory is more accurate than radiative diffusion, it is more cumbersome, and itself is affected by the convection model used (VandenBerg et al. 2008). After we understand the convection problem better, this approach can be extended by a more sophisticated multi-dimensional treatment of radiative transfer in the outer regions. Comparison to three-dimensional hydrodynamic atmospheres (e.g., Stein & Nordlund 1998; Nordlund & Stein 2000; Nordlund et al. 2009) can test the validity of this approach.

2.2. Standard Input Physics

These computations were done using the TYCHO stellar evolution code (revision 12; version control by SVN). Opacities were from Iglesias & Rogers (1996) and Alexander & Ferguson (1994) with Grevesse & Sauval (1998) abundances. The OPAL-EOS (Rodgers et al. 1996) equation of state was used over the range of conditions relevant here. The Timmes & Swesty (2000) equation of state is automatically used for higher densities and temperatures, with a smooth interpolation across the joining region. The formulation of MLT is from Kippenhahn & Weigert (1990), with the modifications via the dimensionless geometric factor $g_{\rm ML}$ as given in the Appendix; $g_{\rm ML} \equiv 1$ gives conventional MLT. We stress that convection is treated in exactly the same way, with the same parameters, in the interior and

Table 2
Solar Models with MLT

Model	α_{ML}	g_{ML}	$R/R_\odot$	$L/L_\odot$	$r_{CZ}/R_\odot$	He_{surf}	v_m(km s^{-1})
A	1.650	1.0	1.001	1.000	0.7169	0.2379	2.25
B	2.323	42.0	1.001	1.000	0.7172	0.2378	2.80
C	3.286	270.0	1.001	0.9997	0.7173	0.2377	3.05
D	4.000	595.0	1.000	0.9997	0.7168	0.2373	3.20
E	5.190	1540.0	1.001	0.9998	0.7172	0.2377	3.40
Sun	···	···	1.000	1.000	0.713 ± 0.001	0.24	3.20[a]

Note. [a] Inferred from the model data in Asplund et al. (2005).

in the envelope (VandenBerg et al. 2008). Diffusion was treated with the Thoul subroutine (see Thoul et al. 1994); radiative levitation (Michaud et al. 2004) was ignored. The nuclear reactions were solved in a 177 isotope network using Reaclib (Rauscher & Thielemann 2000); weak screening rates were incorporated as in John Bahcall's exportenergy.f program. The changes in metallicity due to nuclear reactions and to diffusion were taken into account by interpolation in both the opacity and the equation of state tables. The same equation of state and opacity tables are used in the interior and the atmosphere.

2.3. Modified MLT Models

We examine the solar models resulting from several choices of the mixing length, each constructed by varying the geometric factor g_{ML} until the correct radius of the present-day Sun was obtained. The other MLT parameters a and b are the flavor ML1 in Table 1.

Five such models were constructed, with values of α_{ML} ranging from 1.6 to 5.2, as summarized in Table 2. The model A has $\alpha_{ML} = 1.643$, $g_{ML} = 1.0$, and is typical of current solar models which use the Eddington gray atmosphere as the outer boundary condition and conventional MLT (e.g., Schlattl et al. 1997). This provides a baseline for comparison. Model D has $\alpha_{ML} = 4.0$, which is most consistent with hydrodynamic simulations.

Arnett et al. (2009) found that α_{ML} was not constant, but depended upon the flow properties and the equation of state. For solar models, the surface convection zone is deep, and changes little, so taking a constant α_{ML} is an adequate approximation for this particular example. In MLT, the velocity obtained by a convective eddy is computed from the work done by the buoyancy force over a mixing length:

$$v_c^2 = \alpha_{ML}^2 g H_P \beta_T (\Delta\nabla)/8, \quad (5)$$

where β_T is the compressibility, H_P is the pressure scale height, and $\Delta\nabla \equiv \nabla - \nabla_{ad}$ is the usual "superadiabatic excess." For a given convective luminosity, larger α_{ML} implies larger velocities.

Shallow convection zones, having shorter distances for buoyant acceleration to work, will have smaller values of α_{ML} and smaller velocity scales (Arnett et al. 2009). As the depth of the convection zone increases, the size of the largest eddies also rises, and the pressure at the (now deeper) bottom increases, implying larger α_{ML}. Such an increase will not continue indefinitely; more vigorous convection develops more violent dissipation. The value of α_{ML} seems to "saturate" for very deep convection zones (Arnett et al. 2009; Meakin & Arnett 2010a, 2010b). The solar convection zone is 20 pressure scale heights deep and has yet to be simulated for its full depth with resolution as high as used in Meakin & Arnett (2007b) or Stein & Nordlund (1998). Here, we will examine the case in which such saturation occurs at $\alpha_{ML} \approx 4$. This may be appropriate for the simulations of Nordlund and Stein (R. Stein 2008, private communication) and those of Meakin & Arnett (2010a, 2010b), and is consistent with the insensitivity of the Stein & Nordlund (1998) simulations to the exact position of the lower boundary, which was deeper than this. Further analysis of this issue is in progress (Meakin & Arnett 2010b); three-dimensional simulations for convective zones of depth 0.5–5 pressure scales heights seem consistent with this interpretation. The distribution of values for α_{ML} in Table 2 covers this range.

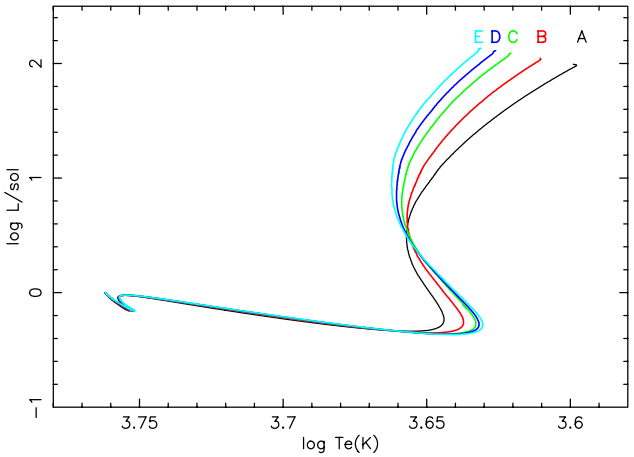

Figure 1. Solar models which differ only by the mixing length and the geometric factor, scaled to have the same radius. The trajectories in the H–R diagram nearly overlay one another except on the Hayashi track, where they are poorly constrained. Note that the stellar birthline (Stahler & Palla 2004) lies near $\log L/L_\odot \approx 1$; the more luminous parts of the tracks ignore accretion and so are not realistic.

(A color version of this figure is available in the online journal.)

Softer equations of state, such as in partial ionization zones or electron–positron pair zones, give less vigorous velocities, but do not change the qualitative picture (Arnett et al. 2009). The simulations of Porter & Woodward (2000), for an ideal gas equation of state, also seem to suggest that saturation may be beginning around $\alpha_{ML} \approx 3$, which is consistent.

Figure 1 shows the evolutionary tracks in the Hertzsprung–Russell diagram (H–R), for each of the models (which differ only by the α_{ML} and g_{ML} parameters). For each α_{ML}, a value of g_{ML} is chosen which gives a reasonable radius for the present-day Sun. After passing the stellar birthline (deuterium burning, $L \approx 10\,L_\odot$; see Stahler & Palla 2004), the tracks are very similar for all five models. However, the increasing values of α_{ML} imply increasing turbulent velocities (Equation (5)). Table 2 gives values of the radius ($R/R_\odot$), luminosity ($L/L_\odot$), the radius of the lower boundary of the convective zone ($r_{CZ}/R_\odot$), the surface (convective zone) abundance of helium by mass fraction (He_{surf}), and the maximum mean turbulent velocity in the convection zone (v_m) in km s^{-1}. The increase in v_m with α_{ML} is clear.

The models were adjusted to radius and luminosity of the present-day Sun to about one part in 10^3 or better, which is sufficient to show accurately the differential effects to be discussed here.

It is well known that once a calibration of MLT parameters is done to fit the solar radius, paths in the H–R diagram are little affected by which parameters were used (Pedersen et al. 1990; Salaris & Cassisi 2008). However, the variation of the velocity scale, although noticed by Pedersen et al. (1990) for example, has not been stressed. In Table 2, it is striking that

only the velocity scale varies significantly with the variation of $\alpha_{\rm ML}$ and $g_{\rm ML}$ pairs constrained to fit the radius and luminosity of the present-day Sun. This velocity scale is crucial for rates of entrainment, wave generation, and mass loss, and so may ultimately cause a change in the evolutionary behavior when such effects are correctly included. It will be argued below that this variation in the velocity scale has direct observational consequences (via line profiles and micro- and macro-turbulent velocities).

The values of the lower radius of the solar convection zone $r_{\rm CZ}$ and the surface helium abundance $\rm He_{surf}$ are slightly different from the values of the standard solar model. Part of the difference may be due to small errors in our stellar evolution code, which is not yet in its fully verified state. However, the standard solar model uses MLT and therefore ignores several significant aspects of convection: turbulent heating, flux of kinetic energy, and entrainment. These effects may move our models toward the inferred values from helioseismology. In any case, the differential effects we discuss here are much larger, and unlikely to be affected by small modifications in the reference model. Note that the predicted values of $r_{\rm CZ}$ and $\rm He_{surf}$ vary in only the fourth significant figure for models A–E, while the velocity scale increases by more than 40%.

3. YREC AND GARCHING SOLAR MODELS

Our solar models are in good agreement with YREC and Garching models, but not yet as close to either as they are to each other.[5] In this paper, we concentrate on the differences caused by changing MLT parameters and outer boundary conditions, rather than finding the absolute best standard solar model. Finding the absolute best solar model requires going beyond present formulations used in YREC and Garching codes (e.g., Michaud et al. 2004; Meakin & Arnett 2007b; Arnett et al. 2009); we plan to address this in detail in future publications.

3.1. Empirical Outer Boundaries

The Yale code (Demarque & Percy 1964; Guenther et al. 1992) uses as an outer boundary condition the empirically derived fit of Krishna Swamy (1966) to the T–τ relation for the Sun, ϵ Eridani, and Gmb 1830. Empirical fits have the flaw that they are suspect if extrapolated; these stars are on the main sequence, and of G and K spectral type (G2V, K2V, and G8Vp, respectively). Gmb 1830 is a halo star of 0.64 $M_\odot$ with a metallicity of about 0.1 of solar (Allende Prieto et al. 2000), while ϵ Eridani is a solar metallicity star of about 0.85 $M_\odot$. If applied to stars of the same stage of evolution and the same abundance, such empirical boundary conditions are at their best. Unfortunately, the "calibration" approach may hide mistakes in the assumed physics.

3.2. Atmospheric Outer Boundaries

The Garching code (Schlattl 1996) was modified (Schlattl et al. 1997) to use synthetic atmospheres fitted to the interior solution at optical depth ($\tau = 20$). In addition, a spatially varying mixing length was employed to reproduce the pressure–temperature stratification calculated by two-dimensional-hydrodynamic models (Freytag et al. 1996). This involved the interpolation between an atmospheric value (Balmer-line fits gave $\alpha_{\rm at} = 0.5$) and an interior value ($\alpha_{\rm int} = 1.7$ to get the correct solar radius); see (Freytag et al. 1996) for details. This approach can be extended with a library of hydrodynamic model atmospheres (and unlike the Yale approach, is not in principle limited to G stars). However, we find that our own two-dimensional simulations, because of the pinning of vortices, do not mix material as efficiently as the three dimensional case. For a given driving, the two dimensional case gives higher velocities to maintain the same convective luminosity (Asplund et al. 2000; Meakin & Arnett 2007a, 2007b). Further, two-dimensional simulations have a different turbulent cascade and damping than the three dimensional case, which is related to this velocity difference. These issues need to be dealt with in making contact between actual convective velocities and observed line widths.

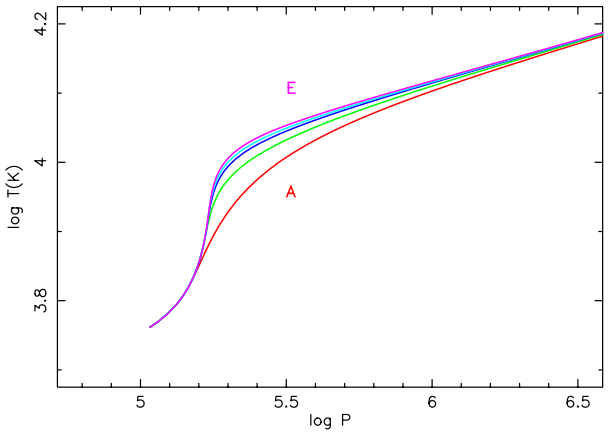

Figure 2. Structure of sub-photospheric regions with different choices of the $\alpha_{\rm ML}$–$g_{\rm ML}$ pairs. Model A is the lowest curve, and models B, C, D, and E are successively higher. Model A is similar to the "Eddington-approximation" case of Schlattl et al. (1997), while models C, D, and E are similar to their "2D-hydro-model" case.

(A color version of this figure is available in the online journal.)

3.3. The Subphotospheric Region

How does changing the $\alpha_{\rm ML}$–$g_{\rm ML}$ pair affect the structure of the sub-photospheric layers? Figure 2 shows models A–E in the log pressure–log temperature plane. This may be directly compared with Figure 1 in Schlattl et al. (1997). Model A is almost identical to their curve labeled "Eddington-approximation," which used radiative diffusion and MLT with conventional parameters (essentially the same as model A, $\alpha_{\rm ML} \approx 1.7$ and $g_{\rm ML} = 1$). In contrast, model D, which also used the Eddington approximation but used MLT with $\alpha_{\rm ML} = 4.0$ and $g_{\rm ML} = 595.0$, closely resembles their curves labeled "2D-hydro-model" and "1D-model-atmosphere," and models C and E are similar. It appears that the significant point is not the choice of radiative diffusion versus radiative transfer, but rather the treatment of convection (VandenBerg et al. 2008). The Yale group get hydrodynamics by empirical fitting to hydrodynamic observed atmospheres, the Garching group get hydrodynamics by a fit to their two-dimensional hydrodynamic atmospheres, and we get hydrodynamics by analytic theory based on three-dimensional simulations of convection.

4. THE SAR AND SURFACE VELOCITIES

4.1. The Geometric Factor $g_{\rm ML}$

Although the traditional procedure for calibrating stellar convection is the variation of the parameter $\alpha_{\rm ML}$ to adjust the

[5] Our goal is to develop a software environment that allows modification of physical modules by logical switches, thus maintaining consistency between old and new implementations. We plan to persist until we have an option that removes even the small differences which remain for the standard solar model.

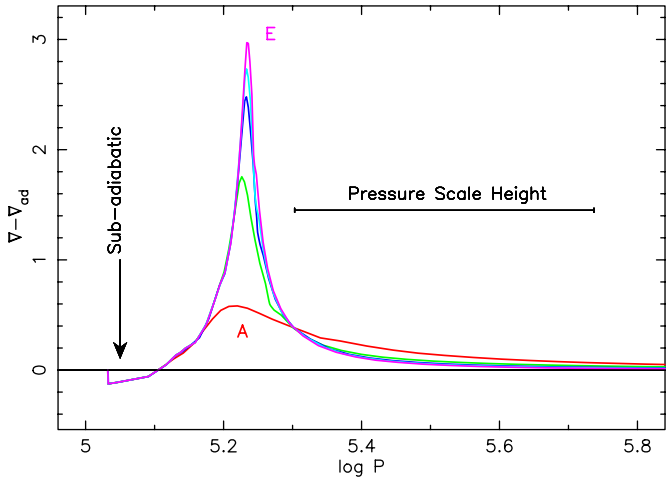

Figure 3. Structure of the SAR, with $\Delta\nabla = \nabla - \nabla_{\rm ad}$ vs. logarithm of pressure (dynes cm^{-2}). The width of the SAR is much less than a pressure scale height; this may be compared with ℓ_b/H_P in Table 2. The small blob size implied in models C, D, and E is consistent with the small width of the SAR, which is all we should expect without a three-dimensional atmospheric model. Note the small sub-adiabatic region just below the photosphere (the left of the graph, indicated by the arrow).

(A color version of this figure is available in the online journal.)

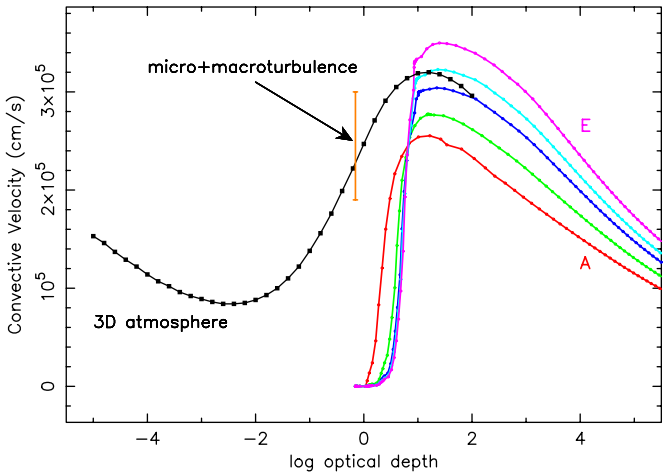

Figure 4. Convective velocities vs. log optical depth for solar models which differ only by the mixing length and the geometric factor. The convective velocity changes while there are no other significant changes; standard MLT with the Schwarzschild criterion was used. Case A had $\alpha_{\rm ML} = 1.643$ and the usual geometric factor, $g_{\rm ML} = 1$. Case D ($\alpha_{\rm ML} = 4$ and $g_{\rm ML} = 595.0$) is the estimated value for saturation of the dissipation length for a solar convection zone of depth of 20 pressure scale heights. In MLT, the velocity scale is not constrained physically, but only fixed by historical parameters (which are inconsistent with both three-dimensional simulations and hydrodynamic theory). The three-dimensional model atmosphere data from Asplund et al. (2005) are dramatically different at small optical depth.

(A color version of this figure is available in the online journal.)

stellar radius keeping $g_{\rm ML}$ constant, this is not the most natural choice. It is $g_{\rm ML}$ that determines the radiative diffusion rate from "convective blobs," and is most effective in the SAR. In the adiabatic regions, MLT gives an adiabatic gradient, so the choice of $\alpha_{\rm ML}$ is irrelevant to structure there. Historically, the reasonable choice—of forcing a one-parameter family by assuming constant values for all parameters except $\alpha_{\rm ML}$—has obscured the physics. Simulations uncovered this mistake, with the indication that $\alpha_{\rm ML}$ is determined by the dissipation which is fed by the turbulent cascade, exactly as Kolmogorov (1941, 1962) suggested.

The geometric factor $g_{\rm ML}$ may be expressed in terms of a ratio of time to transit a mixing length to time for diffusion to remove the superadiabatic excess from a "blob" (Kippenhahn & Weigert 1990). It is not well defined because of geometric vagueness about the "blob"; here, we take it to be proportional to the inverse square of the ratio ℓ_b/ℓ_m, where ℓ_b is the blob diameter and ℓ_m is the mixing length. This is a deviation from MLT, for which $\ell_b \equiv \ell_m$. With this identification, we can compare the SAR thicknesses for different $\alpha_{\rm ML}$–$g_{\rm ML}$ combinations given in Table 2. For model D, we have a full width at half-maximum of the SAR (Figure 3) which is comparable to ℓ_b, which implies consistency within MLT.[6]

This is shown in Table 3. Note that for larger values of mixing length parameter $\alpha_{\rm ML}$, the SAR thickness becomes smaller, whether measured relative to a pressure scale height $\ell_b/H_P = 1/\sqrt{g_{\rm ML}}$ or relative to a mixing length $\ell_b/\ell_m = 1/(\alpha_{\rm ML}\sqrt{g_{\rm ML}})$. This means that, for acceptable solar pairs of $\alpha_{\rm ML}$–$g_{\rm ML}$, larger values of the mixing length imply narrower and more intense SARs to drive the convection. Larger values of mixing length parameter $\alpha_{\rm ML}$ imply larger velocity scale (larger v_m) as Table 2 shows. Thus, models A–E are a sequence having increasingly vigorous and narrowly restricted regions of convective driving (acceleration).

[6] From Figure 3, $\Delta \log P \approx 0.05$–$0.08$, so $\Delta \ln P \approx 0.12$–$0.18$. Model D has $\ell_d/H_P = 0.164$ which is in this range. The weight of this argument is lessened by the conceptual problems with MLT, and the reader is warned against taking these numerical values too literally: the MLT model for the geometric parameter is a very crude representation of the physics.

Table 3
"Blob Sizes" and Mixing Length

Model	$\alpha_{\rm ML}$	$g_{\rm ML}$	ℓ_b/H_P	ℓ_b/ℓ_m
A	1.650	1.0	1.65	1.0
B	2.323	42.0	0.358	0.154
C	3.286	270.0	0.200	0.0608
D	4.000	595.0	0.164	0.0410
E	5.190	1540.0	0.132	0.0255

Figure 3 shows the structure of the SAR for models A–E. This may be compared to Figure 2 of Schlattl et al. (1997). Again model A resembles their "Eddington-approximation" curve, and models C, D, and E are similar to their "2D-hydro-model" and "1D-model-atmosphere" curves. Here $\Delta\nabla \equiv \nabla - \nabla_a$ is plotted against logarithm of pressure (dynes cm^{-2}).

Above the horizontal line $\Delta\nabla = 0$, buoyant forces accelerate the turbulent flow, while below the line we have buoyancy damping (deceleration; this region is barely visible at the left edge of the curve). According to MLT with the Schwarzschild criterion for convection, there should be no flow for $\Delta\nabla \leqslant 0$. The area above (under) the curve gives the net buoyant acceleration (deceleration). Clearly the deceleration, seen as the small depression near $\log P = 5$, is overcome by the much larger region of acceleration around $\log P \approx 5.2$, so that the Schwarzschild criterion gives incorrect results here. The area argument implied in Figure 3 is essentially the bulk Richardson number criterion (Fernando 1991; Meakin & Arnett 2007b), and is nonlocal. Therefore, because the pathological deceleration implied by use of the Schwarzschild criterion is incorrect, the velocities v_m given in Table 2 are directly related to those which produce solar line broadening.

4.2. Micro- and Macro-turbulence

Figure 4 shows the run of turbulent velocity as a function of optical depth for the five models, and for the Nordlund–Stein

three-dimensional hydrodynamic atmosphere quoted in Asplund et al. (2005). The semi-empirical stellar atmosphere models of Fontenla et al. (2006) give curves similar to those of Nordlund–Stein, but are not plotted to reduce crowding. The most striking feature in this figure is the difference between the low depth behavior of the models (an abrupt cliff at $\tau \approx 1$), and the three-dimensional atmospheres (a gentler slope for lower τ). This is due to the use in the one-dimensional models of the Schwarzschild criterion for convection, a local condition. A weakly stable stratification cannot really hold back vigorous motion, as use of the local Schwarzschild criterion implies.

The micro- and macro-turbulent velocities, $\zeta_{\rm mi}$ and $\zeta_{\rm ma}$, are parameters which were introduced long ago[7] to account for the embarrassment that, according to the Schwarzschild criterion, conventional solar atmospheres are *not* convective at the surface. Note that if $\zeta = \sqrt{\zeta_{\rm mi}^2 + \zeta_{\rm ma}^2}$, then $1.9\,{\rm km\,s^{-1}} \leqslant \zeta \leqslant 3.0\,{\rm km\ s^{-1}}$ for the Sun (Cox 2000). This is indicated by the vertical bounded line in Figure 4. The connection between this ζ and the actual turbulent velocity due to convection is not simple, involving line-formation, photon escape, and inhomogeneous stellar surface layers.

Fortunately, multi-dimensional hydrodynamic atmospheres (Asplund 2000; Nordlund & Stein 2000) do provide a spectacular fit to line shapes, with no free parameters, so we identify the convective velocities well below the photosphere (optical depth $\tau \gtrsim 3$) in these simulations with those predicted by our hydro-dynamically consistent choice of mixing length parameter $\alpha_{\rm ML}$. This means we are essentially matching different three-dimensional simulations in the region of adiabatic convection, where they should give identical answers, and minimizing the sensitivity of the match to the complexities of atmospheric detail. Optical depth is sensitive to temperature (the opacity is $\kappa \propto T^{10}$ here), so that the visible surface is a complex structure (see Figure 24 in Stein & Nordlund 1998). For example, a 10% fluctuation in temperature implies a change in 2.4 in the opacity. The optical depth of the photosphere occurs at different radii for different positions on the solar surface, so that fitting it with a single radius is difficult. At greater depths we expect the three-dimensional atmospheres and the one-dimensional models to agree, but near the surface it is not clear that the three-dimensional and one-dimensional definitions of optical depth are consistent.

Pressure should be a better coordinate for matching three-dimensional results to a one-dimensional model. Unlike the optical depth, the pressure is a weaker function of angular position on the solar surface. Hydrodynamic flow tends to smooth pressure variations, making the definition of a mean pressure–radius relation more meaningful. Figure 5 plots convective velocities versus log pressure for models A–E. We can see that the Asplund et al. (2005) model smoothly joins onto model D.

Let us construct a simple model of the motion in this region to see how hydrodynamic arguments might give modifications to the purely hydrostatic boundary conditions used in models A–E. We will assume that the velocity is dominated by flow at the largest scales of turbulence. These scales contain most of the kinetic energy and are least non-laminar. Convective motions are driven by the sinking of matter which is cooling due to transparency near the surface. This generates gravity waves in the near-surface region. We will approximate the large-scale average of this motion by g-modes (Landau & Lifshitz

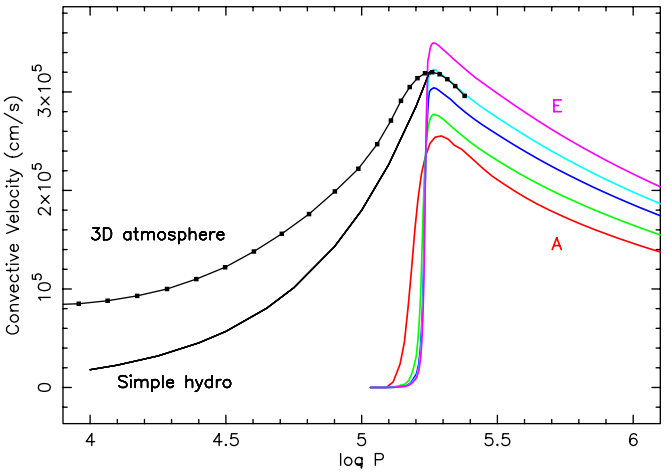

Figure 5. Convective velocities vs. log pressure, for solar models and three-dimensional hydrodynamic solar atmospheres. The atmospheres extend to lower pressure than the solar models (actually the atmospheres extend to higher pressure too, but these values were not in Table 1 of Asplund et al. 2005). It is clear that the three-dimensional atmospheres would join smoothly onto solar model D for $\alpha_{\rm ML} = 4.0$ and $g_{\rm ML} = 595.0$, as we would have predicted. The thin solid curve labeled "Simple hydro" represents a hydrodynamic extrapolation from the point of maximum convective velocity (see the text). Replacing the MLT estimate (based on the Schwarzschild criterion and hydrostatic structure) with a physically motivated estimate gives a strikingly better agreement with both the three-dimensional atmospheres and the empirical solar data.

(A color version of this figure is available in the online journal.)

1959, see Section 12) whose amplitude falls off exponentially with pressure scale height. This implied a scaling with position above an interface at radius r_0, $P(r) = P(r_0)v(r)/v(r_0)$. Despite its extreme simplicity and harsh assumptions, this simple picture gives a significantly improved approximation to the behavior of the velocity in the photospheric regions. The thin black line labeled "Simple hydro" in Figure 5 represents such flow, fitted from the point of maximum convective velocity in model D. It captures the qualitative behavior far better than the conventional hydrostatic assumptions (shown as the steep "cliff" near $\log P = 5.25$), and promises to do better as the complex physics of the photosphere is more faithfully represented (Stein & Nordlund 1998; Nordlund & Stein 2000).

This suggests that the photospheric velocity may be estimated by $\zeta \approx 0.8\ v_m$, which predicts a connection between fitted line shapes and convective flow. Better physics for turbulent flow seems to be needed in one-dimensional stellar atmospheres, and some three-dimensional features are difficult to represent in one dimension, such as inhomogeneity between upward and downward moving flows (Stein & Nordlund 1998; Nordlund & Stein 2000; Steffen 2007). The three-dimensional hydrodynamic atmospheres can provide insight into the correct mapping of realistic physics of a multi-modal region onto a one-dimensional stellar model, and tighter constraints on ζ for a given v_m. For models A–E, this condition favors model D.

Independent of any estimate of ζ, our simulations and theory (Meakin & Arnett 2007b; Arnett et al. 2009) suggest from hydrodynamics alone that models C, D, and E are most plausible, i.e., $\alpha_{\rm ML}$ lies in the range of 3–5 because of enhancement of turbulent damping in deeply stratified convection regions ($\alpha_{\rm ML}$ "saturation"). This consistency is encouraging.

4.3. A Sanity Check for MLT

We have found that it is possible to use a hydro-dynamically reasonable value for the mixing length parameter $\alpha_{\rm ML}$ if we

[7] See Huang & Struve (1960) for an early review, in which ζ is already a well-established parameter.

adjust the geometric parameter $g_{\rm ML}$ appropriately. Do these adjusted values make any sense in the mixing-length picture of convection?

In MLT, the geometric factor is related to the "luminosity of a blob" compared to the time it takes a blob to move through its own length: see Kippenhahn & Weigert (1990, p. 43). To estimate the time for excess radiation to leak from the blob, an average opacity for the blob is used. In order for this to be valid, the length of the blob must be much less than the opacity scale height. The geometric factor is only relevant in the SAR, where $\kappa \propto T^{10}$, so that the opacity scale height is $H_\kappa \approx 0.1 H_T$, and thus much *smaller* than the temperature scale height. Figure 2 shows that in the SAR, the temperature scale height is much *smaller* than the pressure scale height. The conventional notion that the MLT blob has a size of the order of a pressure scale height implies that the assumption of an average opacity is violated by much more than an order of magnitude. The relevant physical picture is not a leaky box, but a recombination wave.

It seems fortuitous that the shape of the one-dimensional SAR shown in Figure 3 actually resembles the time-averaged behavior, projected onto the radial coordinate, seen in the three-dimensional atmospheres; see[8] Figure 3 in Nordlund et al. (2009). This good fortune occurs because the average effect of radiation cooling on the entropy of the flow, as it moves through this region of space, is approximately the same as the particular choices of the $g_{\rm ML}$ give. Development of a more accurate physical model than MLT provides is desirable, and three-dimensional atmospheres suggest how this can be done.

5. SUMMARY

Some of the insights from three-dimensional compressible convection simulations and theory (Meakin & Arnett 2007b; Arnett et al. 2009) have been applied to sub-photospheric regions of solar models. Even within MLT, a dynamically consistent velocity field (i.e., a consistent choice of $\alpha_{\rm ML}$ and an adjusted $g_{\rm ML}$), gives a better agreement with

1. empirical $T(\tau)$ relations;
2. three-dimensional hydrodynamic models of stellar atmospheres.

As a bonus we find that by fixing $g_{\rm ML}$ by requiring the MLT "blob" size be consistent with the thickness of the SAR (defined as full width at half-maximum) leaves us with no free MLT parameters.

Using the correct condition for mixing (the bulk Richardson number) implies that the one-dimensional atmospheres should exhibit hydrodynamic flow. Further, simple hydrodynamic considerations (Press 1981; Press & Rybicki 1981) suggest g-mode waves will be generated and penetrate to the photosphere (these are generated by turbulent forcing from convection). We show that there is a connection between the predicted turbulent velocity scale and the observed (macro and micro)-turbulent velocities, which removes the embarrassment of rigorously static surface regions predicted by one-dimensional stellar atmosphere theory.

We may also have a resolution of an apparent contradiction. Atmospheric models of white dwarfs (Winget 2008; Bergeron et al. 1995), which have shallow convection zones, use MLT parameters (ML2: $\alpha = 0.6$, considerably smaller than used for the Sun), indicating less vigorous convection. Low mass eclipsing binaries (Stassun et al. 2008; Morales et al. 2009) are generally fit with $\alpha \sim 1$ (again low convective efficiency), these models do *not* have shallow convection zones. In MLT, there is no rationale for these differences. Use of Equation (1) will give models having thin convection zones which agree with MLT models using small $\alpha_{\rm ML}$, so we expect to reproduce the white dwarf results. For low mass stars, the surface temperatures will be lower than the solar value, so that the SAR should comprise more mass, i.e., we expect larger $g_{\rm ML}$ to be physically correct. Table 2 indicates that there is a trade off between $\alpha_{\rm ML}$ and $g_{\rm ML}$: to compensate for lower $g_{\rm ML}$, α must be lower, for the same radius. For a deep convection zone, $\alpha_{\rm ML}$ is fixed, then a stronger SAR (larger $g_{\rm ML}$, and more inefficient convection) will give a larger radius. This is the sense of the discrepancy of the computed radii for low mass eclipsing binaries (Stassun et al. 2008; Morales et al. 2009), and we suggest that part of the discrepancy may be due to the convection algorithm used. Unfortunately, direct calculation of low mass dwarfs ($M \approx 0.2\,M_\odot$) with $\alpha_{\rm ML} \approx 4$ exposes limitations in MLT: the SAR is forced upward into the photosphere, making three-dimensional atmospheres a necessity for gaining insight into a plausible treatment in stellar models.

We have, in fact, sketched a way to eliminate astronomical calibration from stellar convection theory:

1. Adjust $\alpha_{\rm ML}$ from convection simulations. The mixing length is $\ell_m = \alpha_{\rm ML}\, H_P$ (where H_P is the pressure scale height), and equal to the depth of the convection up to 4 H_P, and $\alpha_{\rm ML} \approx 4$ for deeper convection zones.
2. Adjust $g_{\rm ML}$ from three-dimensional hydrodynamic atmosphere simulations. This is more accurate, and based upon a better physical representation of the phenomenon, but is mathematically analogous to adjusting $g_{\rm ML}$ to reproduce SAR width which is comparable to ℓ_d, i.e., forcing consistency in one-dimension.

Note that a fit to the present-day solar radius is not logically necessary; instead the observed solar radius can provide an independent test of the theory.

By seriously considering MLT, we have determined that no significant free parameters are left to adjust within the framework of the theory. We find that the choice of two characteristic lengths, *which are determined by the flow*, close the system: the turbulent dissipation length and the thickness of the SAR. Alternatively, the constraint that the observed micro- and macro-turbulent velocities agree with those predicted using the bulk Richardson criterion for surface convective mixing can be used instead of the SAR thickness.

MLT is an incomplete theory, but it is suggestive that even modest changes toward a better physical interpretation, based upon three-dimensional simulations and on a more complete turbulence theory, do give improvements in the models. MLT, as used here, may be derived from a more general turbulent kinetic energy equation by ignoring certain terms (Arnett et al. 2009). Some of the ignored terms are important, emphasizing that MLT is incomplete. However, the approach sketched above may be generalized, and inclusion of missing terms gives a convection theory which goes beyond the limits of MLT. The new theory is nonlocal, time-dependent, provides robust velocity estimates, and is based on simulations and terrestrial experiment, with no astronomical calibration. This more difficult theory will be presented in detail in future publications.

[8] Taking a velocity of 3 km s^{-1} allows us to translate their time axis into a space axis; the width of the change in entropy corresponds to a time of 30 s, which implies a spatial dimension of only 10^7 cm. Corrugation of the surface gives a larger time-averaged width.

This work was supported in part by NSF grant 0708871 and NASA grant NNX08AH19G at the University of Arizona. We thank Robert Stein for discussion of his unpublished work on turbulent damping in solar convection simulations, Robert Buchler for discussions on modeling time-dependent convection, and Martin Asplund for providing machine-readable copies of solar surface models.

APPENDIX

MLT GEOMETRIC PARAMETER

This analysis uses the formulation of Kippenhahn & Weigert (1990); see their discussion for more detail. In the MLT, there are two important conditions which involve radiative diffusion: luminosity conservation and blob cooling. The simple condition $L = L(\mathrm{rad}) + L(\mathrm{conv})$ is written as

$$(\nabla - \nabla_e)^{\frac{3}{2}} = \frac{8}{9}U(\nabla_r - \nabla), \tag{A1}$$

which is identical to Equation (7.15) of Kippenhahn & Weigert (1990). Here the subscripts on the ∇'s denote e for mass element (the blob), a for adiabatic, r for radiative, and no subscript for the background (environment) value. The diffusive cooling of the blob implies

$$\nabla_e - \nabla_a = g_{\mathrm{ML}}2U(\nabla - \nabla_e)^{\frac{1}{2}}, \tag{A2}$$

which is identical to Equation (7.14) of Kippenhahn & Weigert (1990), except for the introduction of a scaling factor g_{ML}. For $g_{\mathrm{ML}} \equiv 1$ we regain conventional MLT. Thus, the definition of U becomes

$$g_{\mathrm{ML}}U = \frac{g_{\mathrm{ML}}}{\ell^2}\left[\frac{3acT^3}{\kappa\rho^2 C_P}\left(\frac{8H_P}{g\beta_T}\right)\right], \tag{A3}$$

which is their Equation (7.12) with an extra factor g_{ML}, and our β_T is their δ. If we define $U^* = g_{\mathrm{ML}}U$ and $\zeta^2 = \nabla - \nabla_a + (U^*)^2$, we may write

$$(\zeta - U^*)^3 + \frac{8}{9g_{\mathrm{ML}}}U^*(\zeta^2 - (U^*)^2 - W) = 0, \tag{A4}$$

which is Equation (7.18) of Kippenhahn & Weigert (1990), except for the factor of g_{ML} in the denominator and the replacement of U by U^*. The same solution procedures may now be applied to solve for ζ and hence ∇. Any value of g_{ML} that is not excessively large or small (within a few powers of ten of unity) has no significant effect except in regions that are both convective and nonadiabatic.

An estimate of g_{ML} in terms of the size of a convective "element" or "blob" is given in Table 1 above, which we repeat here: $g_{\mathrm{ML}} = (\ell/\sqrt{3}r_b)^2$, where r_b is the "blob" radius. In MLT, $r_b \equiv \ell/\sqrt{3} \approx 0.577\ell$, forcing two independent length scales, ℓ and $\sqrt{3}r_b$, to be the same.

Adjustment of g_{ML} allows the SAR to have the correct entropy jump, for any reasonable value of the mixing length parameter α_{ML}; that is, α_{ML} may be chosen to be hydrodynamically consistent. This does *not* provide a consistent convective theory if other important effects, such as entrainment and wave generation, are ignored.

REFERENCES

Alexander, D. R., & Ferguson, J. W. 1994, ApJ, 437, 879
Allende Prieto, C., Garcia Lopez, R. J., Lambert, D., & Ruiz Cobo, B. 2000, ApJ, 528, 885
Arnett, D., Meakin, C., & Young, P. A. 2009, ApJ, 690, 1715
Asplund, M. 2000, A&A, 359, 755
Asplund, M. 2005, ARA&A, 43, 481
Asplund, M., Grevese, N., Sauval, A. J., Allende Prieto, C., & Kiselman, D. 2005, A&A, 435, 339
Asplund, M., Ludwig, H.-G., Nordlund, Å., & Stein, R. F. 2000, A&A, 359, 669
Bahcall, J. N. 1989, Neutrino Astrophysics (Cambridge: Cambridge Univ. Press)
Bahcall, J. N., & Pinsonneault, M. H. 2004, Phys. Rev. Lett., 92, 121301
Bahcall, J. N., Serenelli, A. M., & Pinsonneault, M. 2004, ApJ, 614, 464
Balbus, S. A. 2009, MNRAS, 395, 2056
Balbus, S. A., & Hawley, J. F. 1998, Rev. Mod. Phys., 70, 1
Bergeron, P., Saumon, D., & Wesemael, F. 1995, ApJ, 443, 764
Böhm-Vitense, E. 1958, Z. Astrophys., 46, 108
Clayton, D. D. 1983, Principles of Stellar Evolution and Nucleosynthesis (Chicago: Univ. Chicago Press)
Cox, A. (ed.) 2000, Allen's Astrophysical Quantities (4th ed; Melville, NY: AIP)
Cox, J. P. 1968, Principles of Stellar Structure, in two volumes (New York: Gordon & Breach)
Demarque, P., & Percy, J. R. 1964, ApJ, 140, 541
Fernando, H. J. S. 1991, Annu. Rev. Fluid Mech., 347, 197
Fontenla, J. M., Avrett, E., Thuillier, G., & Harder, J. 2006, ApJ, 639, 441
Freytag, B., Ludwig, H.-G., & Steffen, M. 1996, A&A, 313, 497
Grevesse, N., & Sauval, A. J. 1998, Space Sci. Rev., 85, 161
Guenther, D. B., Demarque, P., Kim, Y.-C., & Pinsonneault, M. H. 1992, ApJ, 387, 372
Hansen, C. J., & Kawaler, S. D. 1994, Stellar Interiors. Physical Principles, Structure, and Evolution, XIII (Berlin: Springer)
Huang, S., & Struve, O. 1960, in Stellar Atmospheres, ed. J. Greenstein (Chicago, IL: Univ. Chicago Press), 321
Iglesias, C., & Rogers, F. J. 1996, ApJ, 464, 943
Kippenhahn, R., & Weigert, A. 1990, Stellar Structure and Evolution (Berlin: Springer)
Kolmogorov, A. N. 1941, Dokl. Akad. Nauk SSSR, 30, 299
Kolmogorov, A. N. 1962, J. Fluid Mech., 13, 82
Krishna Swamy, K. S. 1966, ApJ, 145, 174
Landau, L. D., & Lifshitz, E. M. 1959, Fluid Mechanics (London: Pergamon)
Meakin, C., & Arnett, D. 2007a, ApJ, 665, 690
Meakin, C., & Arnett, D. 2007b, ApJ, 667, 448
Meakin, C., & Arnett, D. 2010a, Ap&SS, in press
Meakin, C., & Arnett, W. D. 2010b, ApJ, submitted
Michaud, G., Richard, O., Richer, J., & VandenBerg, D. A. 2004, ApJ, 606, 452
Morales, J. C., et al. 2009, ApJ, 691, 1400
Nordlund, A., & Stein, R. 2000, in ASP Conf. Ser. 203, The Impact of Large-scale Surveys on Pulsating Star Research, ed. L. Szabados & D. Kurtz (San Francisco, CA: ASP), 362
Nordlund, A., Stein, R., & Asplund, M. 2009, Living Rev. Solar Phys., 6, 2
Pedersen, B. B., Vandenberg, D. A., & Irwin, A. W. 1990, ApJ, 352, 279
Porter, D. H., & Woodward, P. R. 2000, ApJS, 127, 159
Press, W. H. 1981, ApJ, 245, 286
Press, W. H., & Rybicki, G. 1981, ApJ, 248, 751
Rauscher, T., & Thielemann, K.-F. 2000, At. Data Nucl. Data Tables, 75, 1
Rodgers, F. J., Swenson, F. J., & Iglesias, C. A. 1996, ApJ, 456, 902
Salaris, M., & Cassisi, S. 2008, A&A, 487, 1075
Schlattl, H. 1996, Diploma thesis, Tech. Univ. Munich
Schlattl, H., Weiss, A., & Ludwig, H.-G. 1997, A&A, 322, 646
Stahler, S. W., & Palla, F. 2004, The Formation of Stars (Weinheim: Wiley)
Stassun, K. G., Hebb, L., López-Morales, M., & Prša, A. 2008, in IAU Symp. 258, Ages of Stars, ed. E. E. Mamajek & D. Soderblom (Cambridge: Cambridge Univ. Press)
Steffen, M. 2007, in IAU Symp. 239, Convection in Astrophysics, ed. F. Kupke, I. Roxburgh, & K. Chan (Cambridge: Cambridge Univ. Press), 36
Stein, R. F., & Nordlund, Å. 1998, ApJ, 499, 914
Tassoul, M., Fontaine, G., & Winget, D. E. 1990, ApJS, 72, 335
Thoul, A. A., Bahcall, J. N., & Loeb, A. 1994, ApJ, 421, 828
Timmes, F. X., & Swesty, F. D. 2000, ApJS, 126, 501
VandenBerg, D. A., Edvardsson, B., Eriksson, K., & Gustafsson, B. 2008, ApJ, 675, 746
Vitense, E. 1953, Z. Astrophys., 32, 135
Winget, D. E., & Kepler, S. O. 2008, ARA&A, 46, 157